

Hydrothermal process used to grow the TiO₂ NB and modify the surfaces, β -amyloid detection mechanism and PEC sensor setup. (Vol. 20, No. 12, see page 6250).

IEEE SENSORS JOURNAL

The IEEE SENSORS JOURNAL is published by the IEEE Sensors Council, which is sponsored by 26 IEEE societies (see the inside back cover). For information please visit <http://www.ieee-sensors.org>. *Member copies of Transactions/Journals are for personal use only.*

Editor-in-Chief (2018-present)

SANDRO CARRARA
Biomedical Circuits & Systems
École Polytechnique Fédérale
de Lausanne (EPFL)
Lausanne, CH-1015 Switzerland

Past Editor-in-Chief (2011-2018)

KRIKOR B. OZANYAN
Photonic Sensors and Systems
Univ. of Manchester
Sch. Elect. & Electron. Eng.
Manchester, M13 9PL U.K.

Past Editor-in-Chief (2009-2011)

EVGENY KATZ
Colloid Science Chemistry
& Biomolecular Sci.
Clarkson Univ.
Potsdam, NY 13699 USA

Past Editor-in-Chief (2003-2009)

H. TROY NAGLE
Electrical & Computer Engineering
NC State Univ.
Raleigh, NC 27695-7115 USA

Founding Editor-in-Chief (2001-2003)

VLADIMIR LUMELSKY
Mechanical Engineering,
Computer Science
Univ. of Wisconsin
Madison, WI 53706 USA

Editorial Board

Associate Editors-in-Chief

GERALD GERLACH
Dresden Univ. of Technol.
Inst. for Solid-State Phys.
01062 Dresden, Germany

Radical Sensors

Topical Editor
CHENG-TA CHIANG
National Chia-Yi University
Chiayi City, Taiwan

Sensor Applications

Topical Editor
SUBHAS C. MUKHOPADHYAY
Macquarie University
Australia

Chemical & Biosensors Sensor Materials

Topical Editor
CAMILLA BARATTO
National Institute
of Optics (INO)
Brescia, Italy

Sensor Phenomena and Modelling

Topical Editor
ZEYNEP CELIK-BUTLER
Univ. of Texas at Arlington
USA

Sensor Interface Electronics

Topical Editor
STOYAN NIHTIANOV
Delft Univ. of Technol.
The Netherlands

Sensor Systems Integration

Topical Editor
MEHMET YUCE
Monash Univ.
Victoria, Australia

Mechanical & Magnetic Sensors

Topical Editor
PAUL C.-P. CHAO
National Chiao Tung Univ.
Hsinchu, Taiwan

Sensor System Networks

Topical Editor
KISEON KIM
Gwangju Inst. Sci. Tech.
Gwangju, 500-712 Korea

Fiber Optic Sensors

Topical Editor
CARLOS RUIZ
Public University Navarra, Spain

Topical Editor-at-Large

JOHN R. VIG
Consultant
33 Bucks Mill Rd.
Colts Neck, NJ 07722 USA

Sensor Data Processing

Topical Editor
MARCO DA SILVA
Universidade Tecnológica
Federal do Paraná
Brazil

QAMMER H. ABBASI
qammer.abbasi@glasgow.ac.uk
M. JALEEL AKHTAR
jaleel.akhtar@ieee.org
MICHAEL ANTONIOU
m.antonio@bham.ac.uk
GIUSEPPE BARILLARO
giuseppe.barillaro@unipi.it
DIEGO RUBÉN BARRETTINO
diego.barrettino@epfl.ch
ARINDAM BASU
arindam.basu@ntu.edu.sg
VENKAT R. BHETHANABOTLA
venkat@eng.usf.edu
ALPER BOZKURT
alper.bozkurt@ncsu.edu
AMITAVA CHATTERJEE
cha.ami@yahoo.co.in
PAI-YEN CHEN
pychen@wayne.edu
BHASKAR CHOUHEY
Bhaskar.Chouhey@eng.ox.ac.uk
TIEN-KAN CHUNG
tkchung@nctu.edu.tw
WAN-YOUNG CHUNG
wychung@pknu.ac.kr
DANILO DEMARCHI
danilo.demarchi@polito.it
WEILEUN FANG
fang@pme.nthu.edu.tw
GIANCARLO FORTINO
g.fortino@unica.it

ELENA GAURA
e.gaura@coventry.ac.uk
BOBY GEORGE
boby@ee.ittm.ac.in
PANTELIS GEORGIOU
pantelis@imperial.ac.uk
SANKET GOEL
sgoel@hyderabad.bits-pilani.ac.in
PROSANTA GOPE
prosanta.nitdgp@gmail.com
DONGSOO HAR
dshar@kaist.ac.kr
SHYQYRI HAXHA
shyqyri.haxha@beds.ac.uk
SHIH-CHIA HUANG
schuang@ntut.edu.tw
AGOSTINO IADICICCO
iadiccico@uniparthenope.it
TARIKUL ISLAM
tislam@jmi.ac.in
BERNHARD JAKOBY
bernhard.jakoby@jku.at
MEHDI JAVANMARD
mehdi.javanmard@rutgers.edu
ABHISHEK KUMAR JHA
abhishek.jha@pg.edu.pl
OKYAY KAYNAK
okay.kaynak@boun.edu.tr
TAN YEN KHENG
tanyenkheng@ieece.org
CHANG-SOO KIM
ckim@mst.edu
JURGEN KOSEL
jurgen.kosel@kaust.edu.sa

RICHARD T. KOUZES
richard.kouzes@pnl.gov
GIJS KRIJNEN
gijs.krijnen@utwente.nl
AIME LAY-EKUAKILLE
aime.lay.ekuakille@unisalento.it
SANG-SEOK LEE
slee@ele.tottori-u.ac.jp
HUANG CHEN LEE
huclee@ccu.edu.tw
SHENG-SHIAN LI
ssli@mx.nthu.edu.tw
YONGJIA LI
yongjia.li@infineon.com
LIYOU LI
liyoli331@gmail.com
YU-TE LIAO
yudoliao@nctu.edu.tw
JANICE LIMSON
j.limson@ru.ac.za
YU-CHENG LIN
yuclin@mail.ncku.edu.tw
NITAIGOUR MAHALIK
nmahalik@csufresno.edu
CARLOS MARQUES
carlos.marques@ua.pt
MAHMOUD MERIBOUT
mmeribout@pi.ac.ae
ROSARIO MORELLO
rosario.morello@unirc.it
RAVIBABU MULAVESALA
ravi@iitrr.ac.in
ASHISH PANDHARIPANDE
pashish@gmail.com

MARCO PETROVICH
mnp@soton.ac.uk
OCTAVIAN POSTOLACHE
octavian.postolache@gmail.com
IOANIOS RAPTIS
i.raptis@inn.demokritos.gr
JEAN-MICHEL REDOUTÉ
jean-michel.redoute@uliege.be
FERRAN REVERTER
ferran.reverter@upc.edu
CHRISARREE ROYCHAUDHURI
chiroosreepram@gmail.com
STEFAN RUPITSCH
stefan.rupitsch@lse.eei.uni-erlangen.de
PIOTR SAMCZYNSKI
psamczyn@elka.pw.edu.pl
THILO SAUTER
sauter@ict.tuwien.ac.at
KAZUAKI SAWADA
sawada@ee.tut.ac.jp
EDWARD SAZONOV
esazonov@eng.ua.edu
EMILIANO SCHENA
e.schena@unicampus.it
ANUJ KUMAR SHARMA
anujsharma@nitdelhi.ac.in
JOSEPH SHOR
joseph.shor@biu.ac.il
GYMAMA SLAUGHTER
gslaught@umbc.edu
PAUL SOTIRIADIS
pps@ieece.org
CHAO TAN
tanchao@tju.edu.cn
ZHICHAO TAN
zhichao.tan@analog.com

IRENE TAURINO
irene.taurino@gmail.com
KEA-TIONG (SAMUEL) TANG
kttang@ce.nthu.edu.tw
GUI YUN TIAN
g.y.tian@ncl.ac.uk
TAKASHI TOKUDA
tokuda@ms.naist.jp
KAĞAN TOPALLI
kagan.topalli@gmail.com
DANIELE TOSI
daniele.tosi@nu.edu.kz
MARKO VAUHKONEN
marko.vauhkonen@uef.fi
CHANG-HEE WON
cwon@temple.edu
QIANG WU
qiang.wu@northumbria.ac.uk
SHANHONG XIA
shxia@mail.ie.ac.cn
RUQIANG YAN
yanruqiang@xjtu.edu.cn
EUI-HYEOK YANG
ehyang@stevens.edu
MINGHONG YANG
minghong.yang@whut.edu.cn
YING ZHANG
yzhang@gatech.edu
YONGQIANG ZHAO
zhaoyq@nwpw.edu.cn
YONG ZHU
y.zhu@griffith.edu.au

TOSHIO FUKUDA, *President*
SUSAN K. "KATHY" LAND, *President-Elect*
KATHLEEN A. KRAMER, *Secretary*
JOSEPH V. LILLIE, *Treasurer*
JOSÉ M. F. MOURA, *Past President*

ALFRED E. "AL" DUNLOP, *Director, Division I*

IEEE Officers

STEPHEN M. PHILLIPS, *Vice President, Educational Activities*
TAPAN K. SARKAR, *Vice President, Publication Services and Products*
KUKJIN CHUN, *Vice President, Member and Geographic Activities*
ROBERT S. FISH, *President, Standards Association*
KAZUHIRO KOSUGE, *Vice President, Technical Activities*
JAMES M. CONRAD, *President, IEEE-US*

IEEE Executive Staff

STEPHEN P. WELBY, *Executive Director & Chief Operating Officer*

THOMAS SIEGERT, *Business Administration*
JULIE EVE COZIN, *Corporate Governance*
DONNA HOURICAN, *Corporate Strategy*
JAMIE MOESCH, *Educational Activities*
SOPHIA A. MUIRHEAD, *General Counsel & Chief Compliance Officer*
LIESEL BELL, *Human Resources*
CHRIS BRANTLEY, *IEEE-USA*

CHERIF AMIRAT, *Information Technology*
KAREN HAWKINS, *Marketing*
CECELIA JANKOWSKI, *Member and Geographic Activities*
VACANT, *Publications*
KONSTANTINOS KARACHALIOS, *Standards Association*
MARY WARD-CALLAN, *Technical Activities*

IEEE Publishing Operations

Senior Director, Publishing Operations: DAWN MELLEY
Director, Editorial Services: KEVIN LISANKIE *Director, Production Services:* PETER M. TUOHY
Associate Director, Editorial Services: JEFFREY E. CICHOCKI *Associate Director, Information Conversion and Editorial Support:* NEELAM KHINVASARA
Senior Manager, Journals Production: PATRICK KEMPF *Journals Production Manager:* EILEEN MCGUINNESS

IEEE SENSORS JOURNAL (ISSN 1530-437X) is published semimonthly by The Institute of Electrical and Electronics Engineers, Inc. Responsibility for the contents rests upon the authors and not upon the IEEE, the Society/Council, or its members. **IEEE Corporate Office:** 3 Park Avenue, 17th Floor, New York, NY 10016-5997. **IEEE Operations Center:** 445 Hoes Lane, Piscataway, NJ 08854-4141. **NJ Telephone:** +1 732 981 0060. **Price/Publication Information:** To order individual copies for members and nonmembers, please email the IEEE Contact Center at contactcenter@ieee.org. (Note: Postage and handling charge not included.) Member and nonmember subscription prices available upon request. **Copyright and Reprint Permissions:** Abstracting is permitted with credit to the source. Libraries are permitted to photocopy for private use of patrons, provided the per-copy fee of \$31.00 is paid through the Copyright Clearance Center, 222 Rosewood Drive, Danvers, MA 01923. For all other copying, reprint, or republication permission, write to Copyrights and Permissions Department, IEEE Publications Administration, 445 Hoes Lane, Piscataway, NJ 08854-4141. Copyright © 2020 by The Institute of Electrical and Electronics Engineers, Inc. All rights reserved. IEEE prohibits discrimination, harassment and bullying. For more information visit <http://www.ieee.org/nondiscrimination>. Printed in U.S.A.

IEEE

SENSORS JOURNAL

JULY 15, 2020

VOLUME 20

NUMBER 14

ISJEAZ

(ISSN 1558-1748)

SPECIAL ISSUE ON PAPERS FROM THE IEEE FLEPS CONFERENCE 2019

GUEST EDITORIAL

Special Issue on Papers From the IEEE FLEPS Conference 2019	
..... R. Dahiya, Z. Celik-Butler, and L. G. Occhipinti	7493

FEATURED ARTICLE

Chemical and Biological Sensors
Microdroplet-Based Organic Vapour Sensor on a Disposable GO-Chitosan Flexible Substrate
M. Bhattacharjee, A. Vilouras, and R. Dahiya
See page 7494

SPECIAL ISSUE PAPERS

<i>Sensor Materials and Solid-State Sensors</i>	
Fe _x Ni _(1-x) O/NiO Heterojunction-Based Selective VOC Sensor Device by Using Temperature Tunability	
..... S. Dey, S. Santra, S. K. Ray, and P. K. Guha	7503
Nanocomposite Zn ₂ SnO ₄ /SnO ₂ Thick Films as a Humidity Sensing Material	
..... M. V. Nikolic, M. P. Dojcinovic, Z. Z. Vasiljevic, M. D. Lukovic, and N. J. Labus	7509
Development of a Fluorinated Graphene-Based Resistive Humidity Sensor	
..... S. Hajian, X. Zhang, P. Khakbaz, S.-M. Tabatabaei, D. Maddipatla, B. B. Narakathu, R. G. Blair, and M. Z. Atashbar	7517
<i>Thermal Sensors</i>	
Printed Temperature Sensor Based on PEDOT: PSS-Graphene Oxide Composite	
..... M. Soni, M. Bhattacharjee, M. Ntagios, and R. Dahiya	7525
<i>Optoelectronic/Photonic Sensors</i>	
UV Phototransistors-Based Upon Spray Coated and Sputter Deposited ZnO TFTs	
..... D. Kumar, T. C. Gomes, N. Alves, L. Fugikawa-Santos, G. C. Smith, and J. Kettle	7532
OLED-OPD Matrix for Sensing on a Single Flexible Substrate	
..... I. Titov, M. Köpke, N. C. Schneidewind, J. Buhl, Y. Murat, and M. Gerken	7540
<i>Fiber-Optics Sensors</i>	
Textile Multitouch Force-Sensor Array Based on Circular and Non-Circular Polymer Optical Fibers	
..... C.-A. Bunge, J. P. Kallweit, M. Al Hour, B. Mohr, A. Bërziòš, C. Grauberger, P. Adi, and T. Gries	7548

(Contents Continued on Page 7490)

<i>Sensor-Actuators</i>	
A PVDF/Au/PEN Multifunctional Flexible Human-Machine Interface for Multidimensional Sensing and Energy Harvesting for the Internet of Things	Y. Dai, J. Chen, W. Tian, L. Xu, and S. Gao 7556
<i>Sensor Phenomenology</i>	
Organic Current Mirror PUF for Improved Stability Against Device Aging	Z. Qin, M. Shintani, K. Kuribara, Y. Ogasahara, and T. Sato 7569
Development of a Flexible Tunable and Compact Microstrip Antenna via Laser Assisted Patterning of Copper Film	S. Masihi, M. Panahi, D. Maddipatla, A. K. Bose, X. Zhang, A. J. Hanson, B. B. Narakathu, B. J. Bazuin, and M. Z. Atashbar 7579
<i>Sensor Modeling</i>	
Radio-Mechanical Characterization of Epidermal Antennas During Human Gestures	C. Miozzi, G. Diotallevi, M. Cirelli, P. P. Valentini, and G. Marrocco 7588
<i>Sensor Systems Integration</i>	
Characterization of On-Foil Sensors and Ultra-Thin Chips for HySiF Integration	M. Elsobky, T. Deuble, S. Ferwana, B. Albrecht, C. Harendt, A. Ottaviani, M. Alomari, and J. N. Burghartz 7595
<i>Sensor Applications</i>	
Laser-Assisted Fabrication of a Highly Sensitive and Flexible Micro Pyramid-Structured Pressure Sensor for E-Skin Applications	V. Palaniappan, S. Masihi, M. Panahi, D. Maddipatla, A. K. Bose, X. Zhang, B. B. Narakathu, B. J. Bazuin, and M. Z. Atashbar 7605

REGULAR ISSUE REVIEW ARTICLES

<i>Fiber-Optics Sensors</i>	
FBG Sensors for Environmental and Biochemical Applications—A Review	M. A. Riza, Y. I. Go, S. W. Harun, and R. R. J. Maier 7614
<i>Sensor Applications</i>	
Visuotactile Sensors With Emphasis on GelSight Sensor: A Review	A. C. Abad and A. Ranasinghe 7628

REGULAR ISSUE PAPERS

<i>Chemical and Biological Sensors</i>	
Real-Time Electrochemical Measurement of N-Acetyl- β -D-Glucosaminidase Activity, Using Redox-Tagged N-Acetyl- β -D-Glucosaminide Hydrolysis as Proof-of-Principle	W. Rernglit, J. Sucharitakul, A. Schulte, and W. Suginta 7639
<i>Mechanical Sensors</i>	
Investigation of High-Sensitivity Piezoresistive Pressure Sensors at Ultra-Low Differential Pressures	M. Basov and D. M. Prigodskiy 7646
The High Frequency Flexural Ultrasonic Transducer for Transmitting and Receiving Ultrasound in Air	L. Kang, A. Feeney, and S. Dixon 7653
<i>Magnetic Sensors</i>	
Non-Magnetization Detection of Arbitrary Direction Defects in Coiled Tubing Based on Fluxgate Sensor	Z. Zhou, J. Zhang, C. Wang, F. Wan, S. He, and R. Yu 7661
Ultrawideband Differential Magnetic Near Field Probe With High Electric Field Suppression	G. Li, W. Shao, R. Chen, X. Tian, Q. Huang, X. Y. Zhang, W. Fang, and Y. Chen 7669
<i>Optoelectronic/Photonic Sensors</i>	
Event-Based Processing of Single Photon Avalanche Diode Sensors	S. Afshar, T. J. Hamilton, L. Davis, A. van Schaik, and D. Delic 7677
Dual-Core Photonic Crystal Fiber-Based Plasmonic RI Sensor in the Visible to Near-IR Operating Band	M. A. Mahfuz, M. A. Hossain, E. Haque, N. H. Hai, Y. Namihira, and F. Ahmed 7692
Surface Plasmon Resonance Sensing Characteristics of Thin Copper and Gold Films in Aqueous and Gaseous Interfaces	E. P. Rodrigues, L. C. Oliveira, M. L. F. Silva, C. S. Moreira, and A. M. N. Lima 7701
Automatic SAR Image Registration via Tsallis Entropy and Iterative Search Process	M.-S. Kang and K.-T. Kim 7711
Online Non-Cooperative Radar Emitter Classification From Evolving and Imbalanced Pulse Streams	J. Sui, Z. Liu, L. Liu, B. Peng, T. Liu, and X. Li 7721

Fiber-Optic Boiling Point Sensor for Characterization of Liquids	<i>J. Hribar and D. Donlagic</i>	7731
<i>Microwave/Millimeter/THz Wave Sensors</i>		
Millimeter-Wave MIMO Array Based on Semi-Circular Topology	<i>H. Cetinkaya, S. Kueppers, R. Herschel, and N. Pohl</i>	7740
A 2-D Radon Transformation for Enhancing the Detection and Imaging of Embedded Defects in Layered Composite Structures Using Millimeter-Wave System ...	<i>N. Vidhya, L. C. Ong, M. Y. Siyal, and M. F. Karim</i>	7750
<i>Fiber-Optics Sensors</i>		
A Pre-Twisted Taper in Dual-Side Hole Fiber for Torsion Measurement With High Sensitivity	<i>Y. Xu, H. Lin, and A. Zhou</i>	7761
<i>Sensor Phenomenology</i>		
UKF Based on Maximum Correntropy Criterion in the Presence of Both Intermittent Observations and Non-Gaussian Noise	<i>Z. Deng, L. Shi, L. Yin, Y. Xia, and B. Huo</i>	7766
Optimization of Reduced GO-Based Cotton Electrodes for Wearable Electrocardiography	<i>S. M. Saleh, S. M. Jusob, F. K. C. Harun, L. Yuliati, and D. H. B. Wicaksono</i>	7774
Validating Commercial Wearable Sensors for Running Gait Parameters Estimation	<i>B. Pairet de Fontenay, J. S. Roy, B. Dubois, L. Bouyer, and J. F. Esculier</i>	7783
<i>Sensor Modeling</i>		
An Improved Fractional-Order Circuit Model for Voltammetric Taste Sensor System With Infused Tea as Analyte	<i>S. Kumar and A. Ghosh</i>	7792
Design and Analysis of GeSn-Based Resonant-Cavity-Enhanced Photodetectors for Optical Communication Applications	<i>S. Ghosh, B. Mukhopadhyay, and G.-E. Chang</i>	7801
<i>Sensor Interface Electronics</i>		
A 126 μ W Readout Circuit in 65 nm CMOS With Successive Approximation-Based Thresholding for Domain Wall Magnet-Based Random Number Generator	<i>G. Narasimman, J. Basu, P. Sethi, S. Krishnia, C. Yi, L. W. Siang, and A. Basu</i>	7810
Ultra-Low Power Human Proximity Sensor Using Electrostatic Induction	<i>H. Fuketa and Y. Morita</i>	7819
Gated Pipelined Folding ADC-Based Low Power Sensor for Large-Scale Radiometric Partial Discharge Monitoring	<i>D. W. Upton, R. P. Haigh, P. J. Mather, P. I. Lazaridis, K. K. Mistry, Z. D. Zaharis, C. Tachtatzis, and R. C. Atkinson</i>	7826
<i>Sensor Data Processing</i>		
Continuous Object Region Detection in Collaborative Fog-Cloud IoT Networks	<i>J. Tang, G. Xiang, D. Guo, and B. Qiu</i>	7837
A Hybrid Method of Remaining Useful Life Prediction for Aircraft Auxiliary Power Unit	<i>X. Liu, L. Liu, D. Liu, L. Wang, Q. Guo, and X. Peng</i>	7848
Direct Position Determination of Moving Sources Based on Delay and Doppler ...	<i>F. Ma, F. Guo, and L. Yang</i>	7859
Pipeline Leak Detection Using Raman Distributed Fiber Sensor With Dynamic Threshold Identification Method	<i>Y. Xu, J. Li, M. Zhang, T. Yu, B. Yan, X. Zhou, F. Yu, J. Zhang, L. Qiao, T. Wang, and S. Gao</i>	7870
Multistatic Passive Radar Sensing Algorithms With Calibrated Receivers	<i>A. Zaimbashi</i>	7878
Seismic Signal Analysis Using Empirical Wavelet Transform for Moving Ground Target Detection and Classification	<i>M. Kalra, S. Kumar, and B. Das</i>	7886
A Multisensor Data Fusion Method for Ball Screw Fault Diagnosis Based on Convolutional Neural Network With Selected Channels	<i>P. Shan, H. Lv, L. Yu, H. Ge, Y. Li, and L. Gu</i>	7896
An Improved Method for the Calibration of a 2-D LiDAR With Respect to a Camera by Using a Checkerboard Target	<i>F. Itami and T. Yamazaki</i>	7906
A Universal Self-Adaption Workspace Mapping Method for Human–Robot Interaction Using Kinect Sensor Data	<i>Y. Tian, G. Wang, L. Li, T. Jin, F. Xi, and G. Yuan</i>	7918
Model-Aided State Estimation of HALE UAV With Synthetic AOA/SSA for Analytical Redundancy	<i>W. Youn, H. S. Choi, H. Ryu, S. Kim, and M. B. Rhudy</i>	7929
An Autonomous Initial Alignment and Observability Analysis for SINS With Bio-Inspired Polarized Skylight Sensors	<i>T. Du, C. Tian, J. Yang, S. Wang, X. Liu, and L. Guo</i>	7941

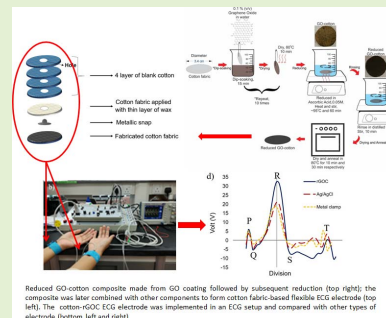
Classification of Atrial Fibrillation and Acute Decompensated Heart Failure Using Smartphone Mechanocardiography: A Multilabel Learning Approach	7957
..... S. Mehrang, O. Lahdenoja, M. Kaisti, M. Jafari Tadi, T. Hurnanen, A. Airola, T. Knuutila, J. Jaakkola, S. Jaakkola, T. Vasankari, T. Kiviniemi, J. Airaksinen, T. Koivisto, and M. Pänkäälä	
Drift-Free Inertial Sensor-Based Joint Kinematics for Long-Term Arbitrary Movements	7969
..... I. Weygers, M. Kok, H. De Vroey, T. Verbeerst, M. Versteyhe, H. Hallez, and K. Claeys	
Robust De-Noising Technique for Accurate Heart Rate Estimation Using Wrist-Type PPG Signals	7980
..... K.R. Arunkumar and M. Bhaskar	
Attitude Estimation of AUVs Based on a Network of Pressure Sensors	7988
..... A. Baruch, Y. Mazal, B. Braginsky, and H. Guterman	
A Deep Learning-Based Ultrasonic Pattern Recognition Method for Inspecting Girth Weld Cracking of Gas Pipeline	7997
..... Y. Yan, D. Liu, B. Gao, G. Y. Tian, and Z. C. Cai	
<i>Sensor Systems Integration</i>	
A Smart Chair Sitting Posture Recognition System Using Flex Sensors and FPGA Implemented Artificial Neural Network	8007
..... Q. Hu, X. Tang, and W. Tang	
Development of Vision Stabilizing System for a Large-Scale Flapping-Wing Robotic Bird	8017
..... E. Pan, X. Liang, and W. Xu	
Measurement of Users' Well-Being Through Domotic Sensors and Machine Learning Algorithms	8029
..... S. Casaccia, L. Romeo, A. Calvaresi, N. Morresi, A. Monteriù, E. Frontoni, L. Scalise, and G. M. Revel	
Geo-Tracing of Black Pepper Using Metal Oxide Semiconductor (MOS) Gas Sensors Array	8039
..... H. E. Lee, Z. J. A. Mercer, S. M. Ng, M. Shafiei, and H. S. Chua	
An Improved PDR/UWB Integrated System for Indoor Navigation Applications	8046
..... S. Guo, Y. Zhang, X. Gui, and L. Han	
Image Dehazing by an Artificial Image Fusion Method Based on Adaptive Structure Decomposition	8062
..... M. Zheng, G. Qi, Z. Zhu, Y. Li, H. Wei, and Y. Liu	
Stretchable Human Machine Interface Based on Smart Glove Embedded With PDMS-CB Strain Sensors	8073
..... W. Dong, L. Yang, and G. Fortino	
Experimental Demonstration of an Anti-Shake Hyperspectral Imager of High Spatial Resolution and Low Cost	8082
..... J. Luo, F. Cai, X. Yao, J. Li, Q. Huang, and S. He	
Pulsed Air-Flow Thermography for Natural Crack Detection and Evaluation	8091
..... X. Lu, G. Tian, J. Wu, B. Gao, and P. Tian	
<i>Sensor Applications</i>	
A Navigation and Pressure Monitoring System Toward Autonomous Wireless Capsule Endoscopy	8098
..... F. N. Alsunaydih, M. S. Arefin, J.-M. Redoute, and M. R. Yuce	
Development of a Motion Sensing System Based on Visual Servoing of an Eye-in-Hand Electrohydraulic Parallel Manipulator	8108
..... S. Chaudhuri, R. Saha, A. Chatterjee, S. Mookherjee, and D. Sanyal	
Facial Biometric System for Recognition Using Extended LGHP Algorithm on Raspberry Pi	8117
..... S. Chakraborty, S. K. Singh, and K. Kumar	
Real-Time Detection of Actual and Early Gait Events During Level-Ground and Ramp Walking	8128
..... S. Sahoo, M. Saboo, D. K. Pratihari, and S. Mukhopadhyay	
A Non-Convex L_1 -Norm Penalty-Based Total Generalized Variation Model for Reconstruction of Conductivity Distribution	8137
..... Y. Shi, X. Kong, M. Wang, Y. Wu, and L. Yang	
A Touch Orientation Classification-Based Force–Voltage Responsivity Stabilization Method for Piezoelectric Force Sensing in Interactive Displays	8147
..... S. Gao, R. Guo, M. Shao, and L. Xu	
Relative Angle Correction for Distance Estimation Using K-Nearest Neighbors	8155
..... I. Madray, J. Suire, J. Desforges, and M. R. Madani	
<i>Sensor System Networks</i>	
A Novel Trilateration Algorithm for RSSI-Based Indoor Localization	8164
..... B. Yang, L. Guo, R. Guo, M. Zhao, and T. Zhao	
Multirate Data Collection Using Mobile Sink in Wireless Sensor Networks	8173
..... C.-Y. Chang, S.-Y. Chen, I.-H. Chang, G.-J. Yu, and D. S. Roy	
<hr/> COMMENTS AND CORRECTIONS	
Corrections to “First-Order Piezoresistive Coefficients of Lateral NMOS FETs on 4H Silicon Carbide”	8186
..... R. C. Jaeger, J. Chen, J. C. Suhling, and L. Fursin	

Optimization of Reduced GO-Based Cotton Electrodes for Wearable Electrocardiography

Syaidah Md. Saleh, Syafiqah Md. Jusob, Fauzan Khairi Che Harun, *Member, IEEE*, Leny Yulianti, and Dedy H. B. Wicaksono^{id}, *Member, IEEE*

Abstract—The quality of Electrocardiography (ECG) signal is dependent on the electrode's performance. Comfort and long-term monitoring are the main benefits of a dry and flexible electrode compared to conventional silver/silver chloride (Ag/AgCl) electrode. The main objective of this study is to develop high performance textile-based electrode by optimizing fabrication method and electrode design. Cotton fabric was dipped into graphene oxide (GO), followed by reduction process to form reduced graphene oxide-cotton (rGOC), where L-ascorbic acid ($C_6H_8O_6$) was used as the reducing agent. Conductivity and skin-electrode interface impedance of the fabricated cotton were characterized using Four-point probe (Van der Pauw) and Potentiostat, respectively. This study focuses on the investigation of electrode design that includes fabrication methods, electrode sizes and shapes. The performance of the reduced GO-based cotton (rGOC) electrode in terms of ECG signal quality was compared to conventional Ag/AgCl electrode and metal clamp under static and dynamic wearable conditions. Results from the conducted experiments show that the fabricated electrode's performance is influenced by dipping time and electrode design, with circle-shape electrode shows the highest conductivity (up to 9k S/m at 1 cm² area) compared to square- and rectangular-shape electrodes (<8k S/m and 14.55 S/m, respectively, at 1 cm² area). The circle-shape rGOC electrode's performed better (SNR 14.85±0.22 dB) than Ag/AgCl electrode (SNR 11.26±0.18 dB) and metal clamp (SNR 12.28±0.72 dB) in capturing static ECG signal. A wearable circle rGOC electrode with 1.7 cm radius performed also similarly under static (SNR 32.60±0.72 dB) and dynamic (SNR 30.27±1.37 dB) ECG monitoring, respectively.

Index Terms—Ascorbic acid, cotton fabric, wearable electrocardiography (ECG), graphene oxide (GO), reduced graphene oxide (rGO).



I. INTRODUCTION

CURRENT high awareness on personal healthcare has inspired many researchers or company to develop various

Manuscript received December 6, 2019; revised January 27, 2020; accepted February 28, 2020. Date of publication March 16, 2020; date of current version June 18, 2020. This work was supported in part by the Ministry of Higher Education Malaysia, Universiti Teknologi Malaysia and Collaborative Research in Engineering, Science & Technology (CREST) under Matching under Grant Q.J130000.3001.01M13 and Grant R.J130000.7301.4B248, and in part by the Swiss German University's Central Research Fund under Grant 02/CRF/SGU/2019. The associate editor coordinating the review of this article and approving it for publication was Prof. Ravinder S. Dahiya. (Corresponding authors: Fauzan Khairi Che Harun; Dedy H. B. Wicaksono.)

Syaidah Md. Saleh, Syafiqah Md. Jusob, and Fauzan Khairi Che Harun are with the School of Biomedical Engineering and Health Sciences, Faculty of Engineering, Universiti Teknologi Malaysia (UTM), Johor Bahru 81310, Malaysia (e-mail: fauzan.khairi@gmail.com).

Leny Yulianti is with the Universitas Ma Chung, Malang 65151, Indonesia.

Dedy H. B. Wicaksono is with the Department of Biomedical Engineering, Faculty of Life Sciences and Technology, Swiss German University (SGU), Tangerang 15143, Indonesia (e-mail: dedy.wicaksono@sgu.ac.id; dedy.wicaksono@gmail.com).

This article has supplementary downloadable material available at <http://ieeexplore.ieee.org>, provided by the authors.

Digital Object Identifier 10.1109/JSEN.2020.2981262

wearable medical devices such as biopotential electrode [1]. Increasing health costs has also created high demand in wearable medical device for pre-diagnostic of disease [2]. Recently, Cardiovascular disease (CVDs) has become the number one cause of death worldwide, where heart failure occurs due to a combination of several risk factors [3]. Such risk factors could have been monitored via non-invasive technique like electrocardiography (ECG) [4]. ECG could accurately reveal heart failures like arrhythmias, which are difficult to detect in single frame of time. Atrial fibrillation, for example, if not detected and treated early, could cause blood clotting and stroke over a period of time [5]. Therefore, long-term continuous ECG signal monitoring of cardiac patients or patient with heart-related problem is necessary [6], [7]. For this purpose, dry electrode has been widely discussed as the alternative electrode for conducting the ECG. Dry non-contact electrode, a capacitive electrode, requires neither ohmic contact to human body, nor any specific preparation, e.g. skin preparation [8]–[10]. But, strong artifact may appear in the captured signal when physical activity occurs [11]. On the other hand, dry contact electrode uses a direct coupling electrode-skin interface which can be improved by the existence of sweat or moisture [12],


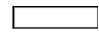



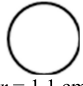

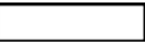
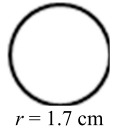
[13]. Textile-based electrode has been a promising dry contact electrode for ECG since it can be made as textile-integrated ECG shirt [14] or a portable multi-sensor heart rate monitor [15]. Textile-based electrodes are also easy to fabricate [16], [17], flexible, lightweight and washable [18], [19].

Textile electrode can be made through several different processes. Recently, Karim *et al.* investigated all inkjet-printed reduced graphene oxide (rGO)-based conductive pattern for e-textile application [20]. Pani *et al.* produced conductive fabric electrode with poly(styrene sulfonate) (Pedot:PSS) using immersing process [21]. Yapici, Alkhdhir *et al.* dipped graphene-clad textile in GO dispersion and performed chemical treatment using reducing agent (hydrogen iodide or hydrazine) to convert the GO into rGO [16]. Other researchers have developed electrode from metal electroplating and deposition [22], [23], screen printing of conductive pastes [24]–[27], sewing or embroidery of metallic threads on fabric [11], [28]–[30], etc. However, no specific studies focusing on the ideal design of wearable ECG electrode have been yet reported. Previously, Karim *et al.* printed about 200 mm × 300 mm electrode on cotton fabric using rGO ink [20], Al Junaibi *et al.* and Pani *et al.* had developed 3 cm × 3 cm square-shape electrode with nylon and polyester fabric, respectively [17], [21]. Yokus and Jur compared three different sizes of circle-shape electrode; $d = 10$ mm, 20 mm and 30 mm [31] for developing non-woven fabric with Ag/AgCl ink as conductive material. Other researchers have embroidered 2 cm × 7 cm size of rectangle-shape electrode using polyethylene terephthalate (PET) yarn coated with Silver/Titanium via sputtering process [11] and 16 mm × 11 mm dimension of active electrode has been fabricated with carbon loaded rubber using stencil printing [26].

Various conductive materials had been used to fabricate textile-based electrode such as PEDOT:PSS [32], Ag/AgCl ink [31] and graphene oxide (GO) [17], [20], [33], [34]. Currently, the benefits of graphene have been extensively discussed due to its outstanding biocompatibility, excellent electric conductivity, superior mechanical properties e.g. elasticity and stiffness, and high thermal conductivity [35]. Graphene or GO can be reduced via chemical reduction or thermal reduction of GO. Chemical reduction was selected here, rather than thermal reduction in order to maintain the textile properties and to prevent any damage. Today, most researchers have chosen ascorbic acid as reduction agent to substitute the more commonly used hydrazine, which is highly toxic and explosive [36]–[38]. Ascorbic acid is environmentally friendly and is one of the most effective reducing agents in restoring π -conjugate (low surface resistance) along with hydrazine (N_2H_4), sodium borohydride ($NaBH_4$), sodium hydrosulfite ($Na_2S_2O_4$) and sodium hydroxide (NaOH) [39].

No study has been found that focuses on the effect of electrode's size and shape to conductivity and skin-electrode impedance, and eventually to the overall ECG performance of the textile electrode. The focus of this paper is then on optimizing the fabrication methods as well as the electrode's size and shape. Flexible and highly conductive electrodes were fabricated by dip-soaking cotton fabric in GO, followed by

TABLE I
DESIGNS FOR TEXTILE-BASED ELECTRODE

Square	Rectangle	Circle	Area, cm^2
 (1 × 1) cm^2	 (0.5 × 2) cm^2	 $r = 0.6$ cm	1
 (2 × 2) cm^2	 (1 × 4) cm^2	 $r = 1.1$ cm	4
 (3 × 3) cm^2	 (2 × 4.5) cm^2	 $r = 1.7$ cm	9

chemical treatment using ascorbic acid to obtain rGO-coated cotton fabric (rGOC). While previous work, by e.g. Karim [20], used an already reduced GO ink to coat textile, in this work we carried out the reduction of the GO *in situ* at the GO-coated fabrics, to fabricate rGO-coated cotton (rGOC), similar to earlier reports by ourselves [40], [41] and others [42]. In addition, the performance of the fabricated textile electrode was compared to conventional Ag/AgCl gelled electrode by calculating and comparing the signal-to-noise ratio (SNR) of the measured ECG signal from the benchmarked electrodes. The fabricated rGOC electrode was also used in wearable ECG measurement for both static and dynamic setup. To the best that we know, this is the first demonstration of the implementation of wearable ECG using rGO-textile electrode.

II. MATERIAL AND METHODS

A. Material Processing

Cotton fabric (100 cm^2) was treated in sodium carbonate (Na_2CO_3 , 0.02 g.ml^{-1} in 100 ml) to remove natural wax of the fabric as well as to improve the capillary absorption properties of the cellulose fibre [43]. 4 mg.ml^{-1} of GO dispersion in water was purchased from Sigma Aldrich Corporation. Distilled water was used to prepare 0.1%(v/v) of GO solution and directly mixed in ultrasonic bath for 1 hour [36], [39]. 0.05 M L-Ascorbic acid ($C_6H_8O_6$) from Sigma Aldrich Corporation was used in chemical reduction for preparing rGO.

B. Sensor Fabrication and Characterization

Three different designs of electrode i.e. circle, square and rectangle, with varying sizes were investigated as shown in Table I. Investigation was conducted on three area sizes: 1 cm^2 , 4 cm^2 and 9 cm^2 . The three variations were implemented for each electrode design as mentioned above. Scoured cotton fabrics having particular design was fabricated according to method from previous works [40], [41] (Fig. S1, supporting information). First, several experiments related to the optimization of dipping time were conducted with method expanded from our previous work [40], [41] and others [42] (Fig. S1, supporting information). The effect of various dipping time, which were 1 min, 5 min, 15 min and 30 min, was

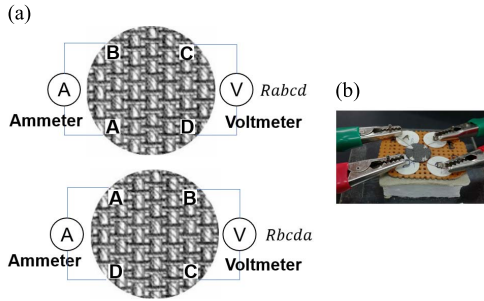


Fig. 1. Two connections of measuring sample resistances (R_{abcd} and $R_{bcd a}$) using Van der Pauw method: (a) schematics; (b) actual setup.

observed based on the measurement of electrical conductivity of the fabricated samples. The optimum dipping time was then used to fabricate different areas and shapes of electrode as shown in Table I. For rectangle shape electrode, the warp of the fabric became the length-side while the weft became the width-side of the shape.

The fabricated samples were characterized using field emission scanning electron microscope (FESEM, Hitachi SU8020) and Energy-dispersive X-ray spectroscopy (EDX) to investigate the morphology of the cotton fibers and the weight percentage of the deposited GO and rGO after fabrication. Raman spectrometer (LABRAM, HR) and X-ray Photoelectron Spectroscopy (XPS) (Kratos) have been used to characterize and distinguish the quality of the fabricated GO Cotton (GOC) and rGOC. The ultraviolet-visible (UV-Vis) reflectance spectra of samples were recorded on a DRUV-Vis spectrophotometer (UV-2700, Shimadzu). Variation in percentage of reflectance spectra indicates the optimum dipping time of the samples and the optimization result was supported with the conductivity measurement. Electrical conductivity of the rGOC was measured with a four-point probe setup (Van der Pauw) shown in Fig. 1 using a source meter (2602B System Source Meter, Keithley) [44], [45]. From Van der Pauw measurement, resistivity, sheet resistance and conductivity, can be calculated. Constant current of 0.5 mA was applied during this measurement.

The conductivity can be calculated using the following formulas,

$$\sigma = \frac{2 \ln 2}{\pi d (R_{abcd} + R_{bcd a}) f(R)} \quad (1)$$

where $f(R)$ is a correction function when $ratio = R_{abcd}/R_{bcd a}$ not equal to 1,

$$f(R) = 1 - \left(\frac{R_{abcd} - R_{bcd a}}{R_{abcd} + R_{bcd a}} \right)^2 \ln 2 - \left(\frac{R_{abcd} - R_{bcd a}}{R_{abcd} + R_{bcd a}} \right)^4 \times \left(\frac{(\ln 2)^2}{4} - \frac{(\ln 2)^3}{12} \right) \quad (2)$$

The formula for the sheet resistance is as follows,

$$R = \rho \frac{L}{A} = \rho \frac{L}{wt} \quad (3)$$

where R is resistance, $\rho = 1/\sigma$ is resistivity, A is cross sectional area, L is length of sample, w is sample width and t is sample thickness.

$$R = \frac{\rho L}{t w} = R_s \frac{L}{w} \quad (4)$$

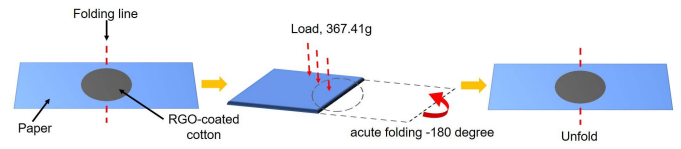


Fig. 2. Experiment illustration of the folding characterization using LCR meter.

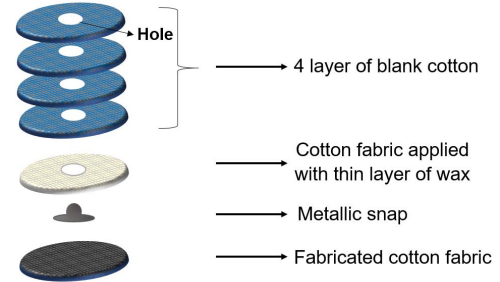


Fig. 3. Schematic diagram of configuration of the electrode.

$R_s = \rho/t$ is the sheet resistance of the coated sample.

C. Sample Characterization, Electrode Fabrication and Testing

1) *Mechanical Characterization (Folding Test)*: The flexibility behavior of fabricated rGOC was examined after several folding tests. The electrical conductivity of rGOC was observed until eight (8) times of folding repetitions through the ratio of conductance-folded to conductance-initial (S/S_0). Initial conductance was recorded before conducting the experiment. The sample was adhered on A4 paper and was folded together at the centre line of the sample (acute folding -180°). A load of ~ 367.41 g was stacked on the folded sample-paper for 5 min and the reading was taken just after the sample-paper was unfolded using LCR meter (Fig. 2). The experiment was repeated until 8 times of folding repetitions.

2) Preparing Reduced Graphene Oxide-Cotton (rGOC)

Electrode: The circle-design electrode was used for further analysis due to its highest value of conductivity from Van der Pauw measurement. Fig. 3 shows the schematic diagram of the electrode configuration. The fabricated rGOC was assembled from several parts of electrode before undergoing electrode testing, thus the quality of signal captured by this new developed ECG electrode could be improved [46]. The metallic snap was adhered at the center of the fabricated cotton fabric (rGOC) electrode using conductive epoxy (CW2400, CIRCUIT WORK, CHEMTRONICS) as a compatible interface to a ECG monitoring system. Single layer of wax-cotton and four layers of blank cotton fabric with the hole at the center were sewn together and sandwiched with the rGO part by an adhesive tape. The purpose of wax-cotton is to make the electrode less stretchable [21] and non-breathable [47] to produce a better quality ECG signal. In addition, four layers of blank cotton were prepared to increase the electrode's thickness. An increased thickness would improve the contact between the electrode and the skin by ensuring a uniform pressure and keeping the electrode wet physiologically through skin contact or artificially [48]. For measuring the impedance of skin-electrode interface, a wire was used to connect the electrode to the measuring device.

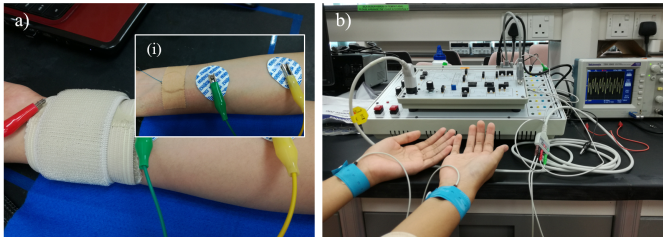


Fig. 4. Electrode testing. a) skin-electrode interface impedance setup with elastic band, wrist support and standard medical adhesive tape (inset image (i)). b) ECG monitoring setup with biomedical measurement system.

3) *Dry Electrode Impedance Measurement*: The quality of ECG signal depends on the impedance of the skin-electrode interface. A small and stable impedance will result in less noise and higher quality signal acquisition. The impedance was inspected using Electrochemical Impedance Spectroscopy (EIS) (Potentiostat VersaSTAT 3). The experiment was carried out to one volunteer, a female subject (Age: 25 years old, BMI: 22). Three electrodes were applied on the inside of the subject's left forearm, where Ag/AgCl commercial electrode was applied as the counter and reference electrodes, and the rGOC was implemented as the working electrode. The distance between the counter and the reference electrodes was set to 8 cm, while that between the reference and the working electrodes was set to 4 cm. The working sense lead was attached together with the working lead electrodes [31]. Standard medical adhesive tape, medical elastic band and wrist support were used to attach the rGOC onto the subject's inside forearm (Fig. 4a) and inset (i)). The Potentiostatic EIS was set to $V_{rms} = 10$ mV and frequency range from 0.1 to 1 kHz. In addition, the subject's skin was cleaned with alcohol swab before experiment was conducted. The applied pressure was maintained by putting the medical elastic band's button at the same position and the wrist support strap (Velcro) at the same marked place.

4) *Sweat Effect and Durability*: To investigate the effect of sweat to the electrode, skin-electrode impedance was measured before 10 minutes and after 25 minutes, recorded from the time it is applied onto the subject's skin. Then to investigate the durability of the rGO binding to cotton, the rGOC was washed using tap water, distilled water and detergent solution (pH 10.65). The conductance was measured after each washing.

D. ECG Monitoring

The performance of the rGOC electrode was then tested using KL-72001 Biomedical Measurement System connected to oscilloscope (TBS 1062, Tektronik). One volunteer, a female subject (Age: 22 years, BMI: 16), was examined using the system and the rGOC electrode, as shown in Fig. 4 (b). Einthoven's Triangle Lead I configuration was chosen to test the performance of the fabricated electrode, where potential across the left arm and right arm was measured. Six (6) samples were prepared for this experiment and six (6) readings were recorded for each set of measurement. Standard medical adhesive tape and medical elastic band were applied to attach the fabric electrode onto both subject's wrists. Prior to electrode placement on the subject's body, alcohol swab was

used to prepare the skin by removing dead skin and grease on the skin. The performance of the rGOC electrode was compared with those of Ag/AgCl and metal clamp commercial electrodes, in terms of signal-noise-ratio (SNR) and ECG waveform. In addition, the electrode's performance in terms of SNR for $r = 1.7$ cm and $r = 0.6$ cm in dynamic condition has also been tested. The ECG signals were recorded using Sichi-ray BMD101 module starter kit (attached with 2 inputs for the electrodes). The electrode device was patched at three places: the center of the manubrium, the top of subject's sternum (left electrode), and 45° diagonals toward left chest (left electrode), using 3M medical adhesive. The device was connected to a smartphone via Bluetooth communication channel (using BMD101 application). The ECG signals were recorded in resting and dynamic conditions where subject was instructed to move her right hand in a toothbrush position (left and right movement, 2 times in a second).

To also investigate the electrode's flexibility, ECG signal was recorded with rGOC electrode using Schiller Medilog FD12plus (Holter system) in both resting (laying on the bed) and dynamic (treadmill) conditions, with 3° inclination and 3 km/h speed.

III. RESULTS AND DISCUSSION

A. Fabricated Sensor

The cotton fabric has a weave pattern that consists of warp and weft directions. To standardize the fabrication of the rectangle shape electrode, warp direction was chosen as the length-side and weft direction for the width-side. Fig. 5 (a) shows that the reflectance spectra ($R\%$) of GOC is higher than that of rGOC. Then, from EDX, the weight percentage of oxygen in the rGOC decreased after reduction (GO: 32% to rGO: 26.545%), while the amount of carbon was increased (Table S1, section S.2 of Supporting Information). This is also confirmed by XPS results which indicates a similar decrease in Oxygen atomic percentage from 41.12% to 24.05% after reduction (Table S2, and the full spectra at section S.3 of Supporting Information). These results are supported by the fact that the electrode's color changes during the GOC to rGOC reduction process, from brown to graphitic black, respectively [49].

From this observation, the scoured cotton fabric was quickly coated with GO dispersion during dipping and drying process due to the occurrence of van der Waals forces and hydrogen bonds between GO and cellulose fibers [39], [50]. FESEM image (10k magnification) in Fig. 5 (b) shows that the cotton fabric was coated homogeneously by GO and no changes of morphological structures of the cotton fibers were observed after fabrication. However, in close-up image (Fig. 5 (b) (i)), a few white spots can be observed in some parts of the fiber due to incomplete exfoliation of graphite particles during the synthesis process [39].

Raman spectroscopy is a multipurpose instrument for characterizing carbon material's structure. Figure 5 (c) shows the variation of D (1345.17 cm^{-1}) and G (1594.82 cm^{-1}) band's intensities of GO and rGO cotton in Raman spectra, respectively, which indicates the change of the electronic conjugation state of GOC during the reduction process [51]. The G band

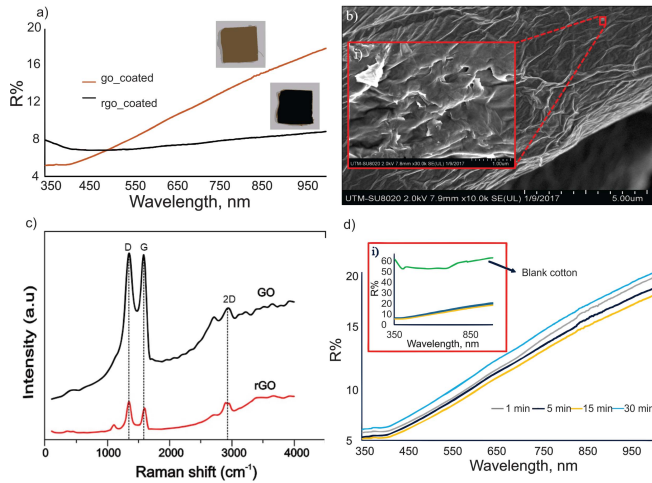


Fig. 5. a) Comparison between GOC and rGO of 15 min dipping time. b) FESEM image for rGO sample of 15 min dipping time and close-up FESEM image (i). c) Raman spectra of GO and rGO cotton fabric. d) Variation of reflectance spectra of rGOC with different cycles of dipping-time; 1, 5, 15, and 30 min. Inset graph (i) with blank cotton. $N = 3$.

corresponds to the sp^2 carbon domain, while the D band corresponds to the sp^3 carbon and defect in graphitic structure or edge planes [37]. The intensity ratio of D and G bands (ID/IG) increased from 1.01 (GOC) to 1.21 (rGOC) upon the reduction. It could be due to the removal of oxygen in GO or the increased segment of graphene edges [52]. These results indicate that rGOC was successfully obtained after the reduction process which has similar agreement with the previous research work [53]–[55].

Generally, variation of dipping time can improve the amount of GO being loaded into the cotton fabric, thus increasing the electrical conductivity of rGOC. Fig. 5 (d) presents the reflectance spectra in the range of 350 nm to 1000 nm wavelength, from GOC made with different dipping times: 1 min, 5 min, 15 min and 30 min. Inset (i) shows that blank cotton (white color) has the highest in reflectance (R%). On the other hand, GOC made with 15 min dipping time shows the lowest percentage of reflectance spectra. Reflectance is inversely proportional to the absorbance, thus sample with 15 min fabrication time has a darker color compared to the other samples. As a result, it has the highest rGO content deposited on the cotton's surface. This data was consistent with the electrical conductivity measurement result shown in Fig. 6 (a).

B. Conductivity

The conductivity of the coated cotton increased when dipping process was carried out 10 times with constant size of electrode (4 cm^2) and constant volume of ascorbic acid (40 ml, 50 mM). The optimum time of dipping process was chosen based on the electrical properties performance of the fabricated cotton. Fig. 6 (a) indicates the electrical conductivity measurement using Van der Pauw method, in which 15 min was found as the optimum time to fabricate rGOC. The electrical conductivity increased from $3916.63 \pm 266.42 \text{ S/m}$ (1 min) to $5890.73 \pm 583.47 \text{ S/m}$ (15 min) and decreased at 30 minutes ($4408.44 \pm 700.24 \text{ S/m}$). This outcome strongly supported

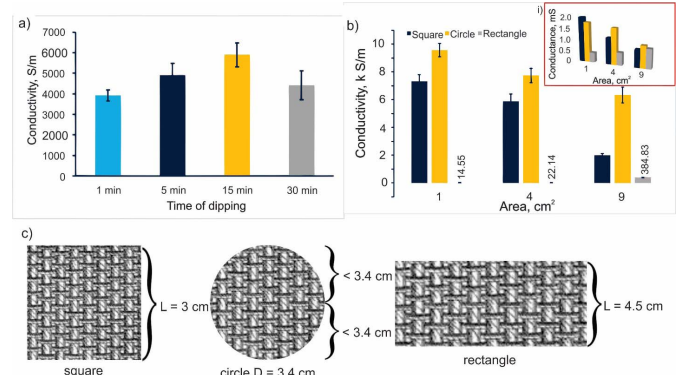


Fig. 6. a) Electrical conductivity measurement using Van der Pauw method (square, 4 cm^2) in optimization of dipping time. $N = 5$ b) Comparison of electrode (square, circle and rectangle) with three different of areas, which are 1 cm^2 , 4 cm^2 and 9 cm^2 . Inset graph (i) conductance measurement using LCR meter. $N = 6$ c) the illustration diagram of thread length for each electrode shape; square, circle and rectangle.

the result of DRUV-Vis characterization in the previous section.

Figure 6 (b) shows conductivity comparison for each of the electrode shapes; square, circle and rectangle with three different sizes using four-point probe (Van der Pauw) and LCR meter (inset (i)). The electrical conductivity performance of square and circle is inversely proportional to the size of electrode. Equation (3) explains that the length of the sample will affect the resistance measurement; small size produces low resistance. However, the rectangle shape electrode indicates an opposite trend. This phenomenon occurred due to the weave properties (weft and warp) of cotton fabric that produced different conductivity value for each direction [44], [47] and also due to the fact that the length-side of weft-warp in rectangle shape electrode is asymmetrical unlike those of the square and circle shape electrodes. Weaving patterns other than common basket weave structure have asymmetrical weaving pattern, which makes their conductivity also varies unequally when shape is changed. In addition, warp and weft thread have different cross section area and different gap between the thread. Warp thread are smaller in diameter and more interwoven gaps, while weft threads have larger diameter and smaller interwoven gaps. When the electrode is made longer in the warp direction, its conductivity will decrease even more compared to if it was made longer in the weft direction.

On average, circle shape electrodes have high conductivity values for various samples with different area: $9,569.59 \pm 483.85 \text{ S/m}$, $7,737.92 \pm 519.97 \text{ S/m}$ and $6,333.82 \pm 581.83 \text{ S/m}$ for 1 cm^2 , 4 cm^2 and 9 cm^2 , respectively. These observations could be due to the variation of the thread length for both weft and warp direction of the circle-shape which allowed the electricity to follow the shortest path (thread), hence decreasing the measurement of resistance. Fig. 6 (c) illustrates the length of the cotton thread in warp direction for each electrode; square, circle and rectangle. The circle shape thread has variation of length (3.4 cm and $< 3.4 \text{ cm}$) and the thread's length decreases when it is farther apart from the circle's diameter. Besides, in ECG monitoring application, the metallic snap is commonly placed at the middle of the electrode. This is understandable since in circular shape electrode,

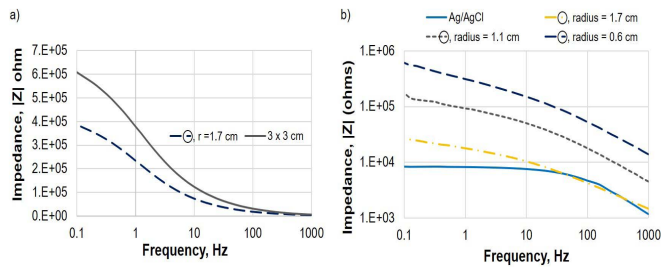


Fig. 7. a) The skin-electrode interface Impedance (Z) of the circle and square shape at 9 cm^2 . b) The skin-electrode interface Impedance (Z) of circle-shape; 1 cm^2 , 4 cm^2 , 9 cm^2 and gelled Ag/AgCl electrode. $N = 6$.

electron from the perimeter of the electrode can travel to the metallic snap at the middle with similar distance. For the square/rectangular shape electrode, electron from the corners of the electrode needs to travel longer distance to the metallic snap. Based on these results, circle shape was chosen for skin-electrode interface impedance analysis.

C. Skin – Electrode Impedance

Prior to the skin-electrode interface impedance measurement of the circle shape electrode, the impedance comparison between two different shapes (square and circle) of the electrode at 9 cm^2 were conducted in light of the conductivity performance results, yet without using the medical elastic band. Fig. 7 (a) illustrates the impedance (Z) performance of square and circle shapes of the electrode at 9 cm^2 using EIS characterization. The results show at 0.1 Hz frequency, the circle shape electrode impedance is lower than that of the square shape electrode, which indicates that it has a better potential to be an ECG electrode. Besides, with the $609.1 \text{ k}\Omega$ (Z), the square shape shows 57% higher impedance compared to the circle shape; $387.6 \text{ k}\Omega$ (Z). The experiments were continued with the three designs of the circle shape and Ag/AgCl electrode with the setup mentioned in the previous section (with medical elastic band). The skin-electrode interface impedance results of circle shape (1 cm^2 , 4 cm^2 and 9 cm^2) and Ag/AgCl electrode are provided in Fig. 7 (b).

As expected, the skin-electrode interface impedance is inversely proportional to the fabricated area [31]. From previous study, the range of impedance measurement for dry-type electrode such as textile and polymer electrode can reach several hundred kilo-ohms to mega-ohms [16], [56]. The skin-electrode interface impedance for gelled Ag/AgCl shows better performance compared to dry fabric electrode, which are $8.3 \text{ k}\Omega$ and $26.4 \text{ k}\Omega$ at 0.1 Hz , respectively. Circle shape electrode having size of 9 cm^2 area has the lowest impedance (Z) compared to other sizes of circle shape electrodes; $174.4 \text{ k}\Omega$ ($r=1.1 \text{ cm}$) and $609.5 \text{ k}\Omega$ ($r = 0.6 \text{ cm}$) at 0.1 Hz . Furthermore, the impedance shows better performance when pressure was applied (with medical elastic band), which resulted in impedance drops from $387.6 \text{ k}\Omega$ to $26.4 \text{ k}\Omega$ at 0.1 Hz . This indicated that the dry-electrode performance will be affected with the pressure exerted on the subject's skin [24], [57]. Although the rGOC electrode has higher skin-electrode interface impedance compared to commercial electrodes, it is still within the acceptable range for dry electrode as observed from previous studies.

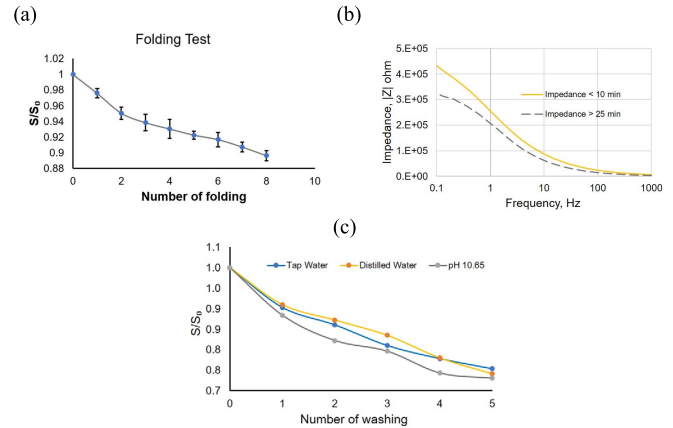


Fig. 8. (a) The changes of sample's conductance after 8 times number of folding. $N = 4$; (b) The skin-electrode impedance before 10 min and after 25 min being applied onto subject skin; (c) The changes of sample's conductance with different types of washing solution and number of washing. $N = 4$.

D. Folding, Sweat and Washing Testing

Fig. 8(a) illustrates the changes of sample's conductance after 8 times of folding for the rGO-coated cotton fabric. The conductance remains 90% even after 8 times of being acutely folded and unfolded repeatedly. This shows that the rGOC is a flexible conductive fabric due to the hierarchical structures of cotton fabric. The GO dispersion is absorbed until the innermost fiber structure of the cotton fabric. The current might flow through thread or fiber structure when the rGO layer on fabric surface cracked during the folding testing. Fig. 8(b) shows the effect of sweat to skin-electrode impedance. The impedance decreased $\sim 24\%$ after being applied $> 25 \text{ min}$, compared to its original value of $432.4 \text{ k}\Omega$ when measured before 10 min of attachment (see details in section S.4 and fig. S4 of Supporting Information).

The adhesion performance of rGO to cotton was examined through washing in various washing liquid as shown in fig. 8(c). Even after 5 times of washing, conductance remains above 70% of the original value (see Supporting Information section S.5 and fig. S5). This shows that rGO binds quite strongly to the textile since there is chemical binding between the GO and the $-\text{OH}$ functional group of the cellulose.

E. ECG Signal

Fig. 9 shows the ECG signal and the SNR acquired from the fabricated rGOC electrode, metal electrode and Ag/AgCl electrode, respectively (see supplementary Excel file and shared research data). The denoising process is first performed using MATLAB software by applying wavelet transform with sym12 as its mother wavelet and 3 levels of decomposition (see supplementary file "function denoised.pdf"). The SNR value is then calculated using the built-in SNR function in the MATLAB software (see supplementary file "SNRcalculation.pdf").

The result clearly revealed that the rGOC (radius = 1.7 cm) electrodes provide better quality of the ECG signal with $14.85 \pm 0.22 \text{ dB}$ (signal-noise-ratio), which is the highest value compared to the performance of Ag/AgCl electrode (gelled area, $r = 0.8 \text{ cm}$) and metal clamp electrode (approximately 9 cm^2 gelled area, depending on subject's wrist

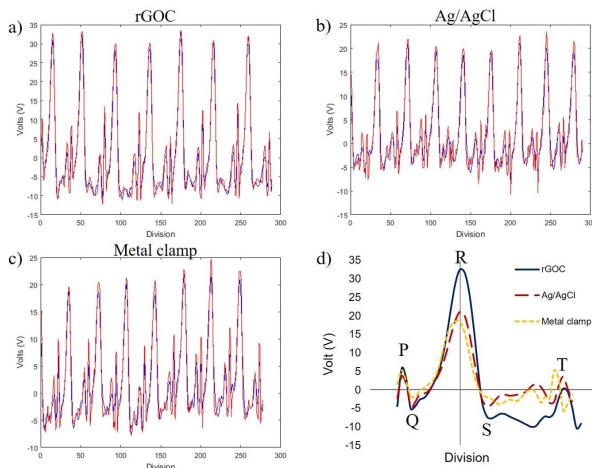


Fig. 9. Superimposed image of raw (red) and denoised (blue) signals acquired using (a) rGO-coated electrode, (b) Ag/AgCl electrode and (c) metal electrode. (d) Overlapped ECG signals of rGOC, Ag/AgCl and metal clamp.

TABLE II

SNR VALUES OF rGOC ELECTRODE, AG/AGCL ELECTRODE AND METAL CLAMP ELECTRODE. N = 6

Electrode	SNR (dB)
Ag/AgCl	11.26±0.18
Metal	12.28±0.72
rGOC	14.85±0.22

TABLE III

SNR READING OF rGOC RADIUS OF 1.7 CM AND 0.6 CM WITH AG/AGCL ELECTRODE USING WEARABLE DEVICE SICHIRAY BMD101 MODULE STARTER KIT. N = 3

Electrode	Size, radius, r (cm)	Resting	Toothbrush motion, SNR, dB
rGOC	1.7	32.60±0.72	30.27±1.37
rGOC	0.6	38.01±3.63	26.34±0.35
Ag/AgCl	0.8	23.52±0.09	26.60±0.01

diameter) (Table II). Results in Table II show that the SNR of the fabricated cotton electrode is 32% and 21% higher than Ag/AgCl and metal clamp electrodes, respectively. Furthermore, the ECG voltage amplitude captured using Ag/AgCl and metal clamp electrodes show deficiency in signal quality since the amplitudes are lower than the signal captured using rGOC cotton electrode (Figure 9 (d)). This result indicates the rGOC cotton electrode provided better electrical performance as an electrode compared to the widely used commercial gelled electrodes (Ag/AgCl and metal clamp electrode). The results proved that rGOC cotton electrode has an excellent potential to measure ECG signal and to produce good signal quality. Thus, this fabricated cotton electrode can be considered to be an alternative for conventional ECG electrode.

Furthermore, Table III indicates the SNR measurement of two different radius of rGOC; $r = 1.7$ cm and $r = 0.6$ cm, and Ag/AgCl electrodes using wearable device Sichiray BMD101 module starter kit on the subject's chest.

The SNR was calculated based on ECG signals acquired in a resting condition and dynamic movement (toothbrush motion) between three (3) electrodes. The result shows that rGOC with 1.7 cm radius provides better signal quality (30.27 ± 1.37 dB) compared to 0.6 cm radius (26.34 ± 0.35 dB) in a dynamic movement. However, the SNR measurement in a rest condition reveal the opposite result outcome and both SNR values are higher relative to dynamic condition. These results are in agreement with the skin-electrode impedance and conductivity measurement where electrode with $r = 1.7$ cm has lower impedance, while the electrode with $r = 0.6$ cm has the highest impedance, respectively. Other than that, the SNR value is higher compared to the previous ECG signals shown in table II due to the distance between two electrodes and the placement of the electrodes. Furthermore, in static condition rGOC electrodes still provides better ECG signals than to that Ag/AgCl electrode. During size optimization, the skin-electrode impedance decreases when the size of the electrode increases. This result means that bigger electrode gives more advantage especially in dynamic condition. However, there are limitations to increasing further the size. First, the larger the electrode side, the captured potential will be an averaged potential in that particular region of the body. Second, when the electrodes are too large, and their distance to each other is not that far on the body, then they may touch each other, resulting in insignificant reading of potential difference.

Further implementation results of the rGOC electrodes in wearable ECG using Holter system are shown in Fig. S6 of section S.6 Supporting Information. The figure shows ECG results of the subject when lying in bed (a), and when the subject is walking at 3 km/h speed on a 3° inclined treadmill (b). rGOC electrodes' results are comparable to those obtained using conventional Ag/AgCl electrodes, and their use during dynamic activity does not results in significant performance reduction.

F. General Discussion

The skin-electrode impedance of conventional clinical electrode is lowered by the use of gel. However, this is not suitable for long-term ECG monitoring using wearable dry electrode. Therefore, the only parameters that we can change is the coating parameters, and the geometry of the electrode itself, i.e. the shape and size. We varied the dipping time to affect the coating and then optimized the shape and size of the electrode, to obtain ECG electrode with the best Signal-to-Noise Ratio (SNR). Previous researchers have reported the use of square and rectangular shape ECG electrode. However, there was no mention yet on their clear benefit compared to conventionally used circular-shape electrodes. Hence, we investigated the performance of different electrode shapes. We found out that circular shape electrode has higher conductivity and lower skin-to-electrode impedance compared to square shape one, even when the area is the same. The innovation points of our ECG electrodes are compared in details with previously reported devices in Table S3 of the Supporting Information section S.7, among others with those using graphene from Lou *et al.* [35], Yapici *et al.* [16],

Al Junaibi *et al.* [17], Hallfors *et al.* [33], Celik *et al.* [58], and especially with the most closely related work by Karim *et al.* [20].

IV. CONCLUSION

15 min dipping time was selected as the optimum time to fabricate rGOC for its highest conductivity and lowest percentage of reflectance spectra. Circle shape-electrode provides better conductivity compared to other electrode shapes. Circle shape electrode with 9 cm² area was chosen as the most optimized electrode size for ECG monitoring due to the low skin-electrode interface impedance value and acceptable value of conductivity. The ECG signal performance of the rGOC electrode is better than Ag/AgCl and metal clamp electrodes, in terms of signal-to-noise ratio. This wearable electrode provides good performance in both static and dynamic ECG measurement.

APPENDIX

Supporting information are attached.

ACKNOWLEDGMENT

The authors would like to express their appreciation to Research Management Centre (RMC) and Ibnu Sina Institute for Fundamental Science Studies (IIS), of Universiti Teknologi Malaysia (UTM), Ministry of Higher Education Malaysia, and also Collaborative Research in Engineering, Science & Technology Center (CREST) for supporting and managing this research. DHBW would like to thank Academic Research and Community Service Centre (ARCS) of Swiss German University for managing funding for this research.

REFERENCES

- [1] A. A. Chlaihawi, B. B. Narakathu, S. Emamian, B. J. Bazuin, and M. Z. Atashbar, "Development of printed and flexible dry ECG electrodes," *Sens. Bio-Sens. Res.*, vol. 20, pp. 9–15, Sep. 2018.
- [2] A. Ankhili, X. Tao, C. Cochrane, D. Coulon, and V. Koncar, "Washable and reliable textile electrodes embedded into underwear fabric for electrocardiography (ECG) monitoring," *Materials*, vol. 11, no. 2, p. 256, 2018.
- [3] W. H. Organization. (May 2017). *Cardiovascular Diseases (CVDs)*. [Online]. Available: <http://www.who.int/mediacentre/factsheets/fs317/en/>
- [4] W. J. Tompkins, *Biomedical Digital Signal Processing*. Upper Saddle River, NJ, USA: Prentice-Hall, 1993.
- [5] X. Xiao, K. Dong, C. Li, G. Wu, H. Zhou, and Y. Gu, "A comfortability and signal quality study of conductive weave electrodes in long-term collection of human electrocardiographs," *Textile Res. J.*, vol. 89, no. 11, pp. 2098–2112, Jun. 2019.
- [6] G.-Y. Jeong, M.-J. Yoon, and K.-H. Yu, "Ambulatory ECG monitoring device with ST-segment analysis," in *Proc. ICCAS-SICE*, Aug. 2009, pp. 509–513.
- [7] E. Fung *et al.*, "Electrocardiographic patch devices and contemporary wireless cardiac monitoring," *Frontiers Physiol.*, vol. 6, p. 149, May 2015.
- [8] T. Wartzek, C. Bruser, M. Walter, and S. Leonhardt, "Robust sensor fusion of unobtrusively measured heart rate," *IEEE J. Biomed. Health Informat.*, vol. 18, no. 2, pp. 654–660, Mar. 2014.
- [9] E. Spinelli, M. Haberman, P. García, and F. Guerrero, "A capacitive electrode with fast recovery feature," *Physiol. Meas.*, vol. 33, no. 8, pp. 1277–1288, Aug. 2012.
- [10] Y.-D. Lin, Y.-H. Chien, S.-F. Wang, C.-L. Tsai, H.-H. Chang, and K.-P. Lin, "Implementation of multiple-channel capacitive ECG measurement based on conductive fabric," *Biomed. Eng., Appl., Basis Commun.*, vol. 25, no. 6, Dec. 2013, Art. no. 1350052.
- [11] M. Weder *et al.*, "Embroidered electrode with silver/titanium coating for long-term ECG monitoring," *Sensors*, vol. 15, no. 1, pp. 1750–1759, 2015.
- [12] E. McAdams, "Biomedical electrodes for biopotential monitoring and electrostimulation," in *Bio-Medical CMOS ICs*. Cham, Switzerland: Springer, 2011, pp. 31–124.
- [13] P. J. Xu, H. Zhang, and X. M. Tao, "Textile-structured electrodes for electrocardiogram," *Textile Progr.*, vol. 40, no. 4, pp. 183–213, Dec. 2008.
- [14] S. Kim *et al.*, "Influence of contact pressure and moisture on the signal quality of a newly developed textile ECG sensor shirt," in *Proc. 5th Int. Summer School Symp. Med. Devices Biosensors*, Jun. 2008, pp. 256–259.
- [15] L. Grajales and I. V. Nicolaescu, "Wearable multisensor heart rate monitor," in *Proc. Int. Workshop Wearable Implant. Body Sensor Netw.*, Apr. 2006, p. 4, and 157.
- [16] M. K. Yapici, T. Alkhidir, Y. A. Samad, and K. Liao, "Graphene-clad textile electrodes for electrocardiogram monitoring," *Sens. Actuators B, Chem.*, vol. 221, pp. 1469–1474, Dec. 2015.
- [17] S. A. A. Junaibi *et al.*, "Initial optimization of Graphene coated fabrics for ECG sensors," in *Proc. IEEE 59th Int. Midwest Symp. Circuits Syst. (MWSCAS)*, Oct. 2016, pp. 1–4.
- [18] W. Zeng, L. Shu, Q. Li, S. Chen, F. Wang, and X.-M. Tao, "Fiber-based wearable electronics: A review of materials, fabrication, devices, and applications," *Adv. Mater.*, vol. 26, no. 31, pp. 5310–5336, 2014.
- [19] C. Liao, M. Zhang, M. Y. Yao, T. Hua, L. Li, and F. Yan, "Flexible organic electronics in biology: Materials and devices," *Adv. Mater.*, vol. 27, no. 46, pp. 7493–7527, Dec. 2015.
- [20] N. Karim *et al.*, "All inkjet-printed Graphene-based conductive patterns for wearable e-textile applications," *J. Mater. Chem. C*, vol. 5, no. 44, pp. 11640–11648, 2017.
- [21] D. Pani, A. Dessì, J. Saenz-Cogollo, G. Barabino, B. Fraboni, and A. Bonfiglio, "Fully textile, PEDOT: PSS based electrodes for wearable ECG monitoring systems," *IEEE Trans. Biomed. Eng.*, vol. 63, no. 3, pp. 540–549, Mar. 2016.
- [22] G. Cho, K. Jeong, M. J. Paik, Y. Kwun, and M. Sung, "Performance evaluation of textile-based electrodes and motion sensors for smart clothing," *IEEE Sensors J.*, vol. 11, no. 12, pp. 3183–3193, Dec. 2011.
- [23] N. Lacerda Silva, L. M. Gonçalves, and H. Carvalho, "Deposition of conductive materials on textile and polymeric flexible substrates," *J. Mater. Sci., Mater. Electron.*, vol. 24, no. 2, pp. 635–643, Feb. 2013.
- [24] G. Paul, R. Torah, S. Beeby, and J. Tudor, "The development of screen printed conductive networks on textiles for biopotential monitoring applications," *Sens. Actuators A, Phys.*, vol. 206, pp. 35–41, Feb. 2014.
- [25] L. Rattfält, F. Björefors, D. Nilsson, X. Wang, P. Norberg, and P. Ask, "Properties of screen printed electrocardiography smartware electrodes investigated in an electro-chemical cell," *Biomed. Eng. OnLine*, vol. 12, no. 1, p. 64, 2013.
- [26] G. Paul, R. Torah, S. Beeby, and J. Tudor, "Novel active electrodes for ECG monitoring on woven textiles fabricated by screen and stencil printing," *Sens. Actuators A, Phys.*, vol. 221, pp. 60–66, Jan. 2015.
- [27] C. R. Merritt, H. T. Nagle, and E. Grant, "Fabric-based active electrode design and fabrication for health monitoring clothing," *IEEE Trans. Inf. Technol. Biomed.*, vol. 13, no. 2, pp. 274–280, Mar. 2009.
- [28] L. Rattfält, M. Lindén, P. Hult, L. Berglin, and P. Ask, "Electrical characteristics of conductive yarns and textile electrodes for medical applications," *Med. Biol. Eng. Comput.*, vol. 45, no. 12, pp. 1251–1257, Nov. 2007.
- [29] V. Marozas, A. Petrenas, S. Daukantas, and A. Lukosevicius, "A comparison of conductive textile-based and silver/silver chloride gel electrodes in exercise electrocardiogram recordings," *J. Electrocardiol.*, vol. 44, no. 2, pp. 189–194, Mar. 2011.
- [30] M. Stoppa and A. Chiolerio, "Wearable electronics and smart textiles: A critical review," *Sensors*, vol. 14, no. 7, pp. 11957–11992, 2014.
- [31] M. A. Yokus and J. S. Jur, "Fabric-based wearable dry electrodes for body surface biopotential recording," *IEEE Trans. Biomed. Eng.*, vol. 63, no. 2, pp. 423–430, Feb. 2016.
- [32] J. Lidón-Roger, G. Prats-Boluda, Y. Ye-Lin, J. Garcia-Casado, and E. Garcia-Breijo, "Textile concentric ring electrodes for ECG recording based on screen-printing technology," *Sensors*, vol. 18, no. 1, p. 300, 2018.
- [33] N. Hallfors, S. Al Junaibi, K. Liao, M. Ismail, and A. Isakovic, "Reduced Graphene oxide for the design of electrocardiogram sensors: Current status and perspectives," in *The IoT Physical Layer*. Cham, Switzerland: Springer, 2019, pp. 3–11.

- [34] N. Hallfors *et al.*, "Graphene oxide: Nylon ECG sensors for wearable IoT healthcare—nanomaterial and SoC interface," *Analog Integr. Circuits Signal Process.*, vol. 96, pp. 253–260, Feb. 2018.
- [35] C. Lou *et al.*, "Flexible Graphene electrodes for prolonged dynamic ECG monitoring," *Sensors*, vol. 16, no. 11, p. 1833, 2016.
- [36] M. J. Fernández-Merino *et al.*, "Vitamin C is an ideal substitute for hydrazine in the reduction of Graphene oxide suspensions," *J. Phys. Chem. C*, vol. 114, no. 14, pp. 6426–6432, Apr. 2010.
- [37] K. K. H. De Silva, H.-H. Huang, and M. Yoshimura, "Progress of reduction of Graphene oxide by ascorbic acid," *Appl. Surf. Sci.*, vol. 447, pp. 338–346, Jul. 2018.
- [38] Z. Khosroshahi, M. Kharaziha, F. Karimzadeh, and A. Allafchian, "Green reduction of Graphene oxide by ascorbic acid," in *Proc. AIP Conf.*, 2018, Art. no. 020009.
- [39] M. Shateri-Khalilabad and M. E. Yazdanshenas, "Fabricating electroconductive cotton textiles using Graphene," *Carbohydrate Polym.*, vol. 96, no. 1, pp. 190–195, Jul. 2013.
- [40] S. M. Saleh, S. M. Jusob, N. S. Sahar, N. A. Abdul-Kadir, F. K. C. Harun, and D. H. B. Wicaksono, "Fabrication of cotton fabric as flexible electrode in electrocardiography monitoring," in *Lecture Notes on Multidisciplinary Research and Application*. Malaysia: Malaysia Technical Scientist Association, 2018, pp. 97–106.
- [41] F. K. C. Harun *et al.*, "Electrodes for measuring electrical activity/signals of body," Malaysia Patent PI 2019007768, Dec. 24, 2019.
- [42] Y. Li, Y. Zhang, H. Zhang, T.-L. Xing, and G.-Q. Chen, "A facile approach to prepare a flexible sandwich-structured supercapacitor with rGO-coated cotton fabric as electrodes," *RSC Adv.*, vol. 9, no. 8, pp. 4180–4189, Jan. 2019.
- [43] A. Nilghaz, D. H. Wicaksono, D. Gustiono, F. A. A. Majid, E. Supriyanto, and M. R. A. Kadir, "Flexible microfluidic cloth-based analytical devices using a low-cost wax patterning technique," *Lab Chip*, vol. 12, no. 1, pp. 209–218, 2012.
- [44] M. Tokarska, "Measuring resistance of textile materials based on Van der Pauw method," *Indian J. Fibre Textile Res.*, vol. 38, pp. 198–201, Jun. 2013.
- [45] L. van der Pauw, "A method of measuring specific resistivity and Hall effect of discs of arbitrary shape," *Philips Res. Rep.*, vol. 13, no. 1, pp. 1–9, 1958.
- [46] C. L. Lam, N. N. Z. M. Rajdi, and D. H. B. Wicaksono, "MWCNT/Cotton-based flexible electrode for electrocardiography," in *Proc. IEEE SENSORS*, Nov. 2013, pp. 1–4.
- [47] E. S. Kaappa, A. Joutsen, A. Cömert, and J. Vanhala, "The electrical impedance measurements of dry electrode materials for the ECG measuring after repeated washing," *Res. J. Textile Apparel*, vol. 21, no. 1, pp. 59–71, Mar. 2017.
- [48] J. Löfhede, F. Seoane, and M. Thordstein, "Textile electrodes for EEG recording—A pilot study," *Sensors*, vol. 12, no. 12, pp. 16907–16919, 2012.
- [49] I. Jung, J.-S. Rhyee, J. Y. Son, R. S. Ruoff, and K.-Y. Rhee, "Colors of Graphene and Graphene-oxide multilayers on various substrates," *Nanotechnology*, vol. 23, no. 2, Jan. 2012, Art. no. 025708.
- [50] M. Shateri-Khalilabad and M. E. Yazdanshenas, "Preparation of superhydrophobic electroconductive Graphene-coated cotton cellulose," *Cellulose*, vol. 20, no. 2, pp. 963–972, Apr. 2013.
- [51] J. Zhang, H. Yang, G. Shen, P. Cheng, J. Zhang, and S. Guo, "Reduction of Graphene oxide vial-ascorbic acid," *Chem. Commun.*, vol. 46, no. 7, pp. 1112–1114, 2010.
- [52] L. M. Malard, M. A. Pimenta, G. Dresselhaus, and M. S. Dresselhaus, "Raman spectroscopy in Graphene," *Phys. Rep.*, vol. 473, no. 5, pp. 51–87, 2009.
- [53] J. Zhang, H. Yang, G. Shen, P. Cheng, J. Zhang, and S. Guo, "Reduction of Graphene oxide via L-ascorbic acid," *Chem. Commun.*, vol. 46, no. 7, pp. 1112–1114, 2010.
- [54] X. Zhu, Q. Liu, X. Zhu, C. Li, M. Xu, and Y. Liang, "Reduction of Graphene oxide via ascorbic acid and its application for simultaneous detection of dopamine and ascorbic acid," *Int. J. Electrochem. Sci.*, vol. 7, pp. 5172–5184, 2012.
- [55] I. A. Sahito, K. C. Sun, A. A. Arbab, M. B. Qadir, and S. H. Jeong, "Graphene coated cotton fabric as textile structured counter electrode for DSSC," *Electrochim. Acta*, vol. 173, pp. 164–171, Aug. 2015.
- [56] Y. M. Chi, T.-P. Jung, and G. Cauwenberghs, "Dry-contact and noncontact biopotential electrodes: Methodological review," *IEEE Rev. Biomed. Eng.*, vol. 3, pp. 106–119, 2010.
- [57] L. Beckmann *et al.*, "Characterization of textile electrodes and conductors using standardized measurement setups," *Physiol. Meas.*, vol. 31, no. 2, pp. 233–247, Feb. 2010.
- [58] N. Celik, N. Manivannan, A. Studwick, and W. Balachandran, "Graphene-enabled electrodes for electrocardiogram monitoring," *Nano-materials*, vol. 6, no. 9, p. 156, 2016.



Syaidah Md. Saleh received the B.Eng. and master's degrees in biomedical engineering from Universiti Teknologi Malaysia, Malaysia, in 2011 and 2014, respectively. She is currently pursuing the Ph.D. degree with the Department of Biomedical Engineering, Universiti Teknologi Malaysia, Malaysia. Her research focuses on developing textile-based electrode using rGO as the conductive material and cotton fabric as a substrate for ECG applications.



Syafiqah Md. Jusob received the B.Eng. degree in biomedical engineering from Universiti Teknologi Malaysia, Malaysia, in 2015. She is currently pursuing the master's double degree with the Department of Biomedical Engineering, Universiti Teknologi Malaysia, with research on flexible cotton fabric-based circuitry using rGO for ECG applications.



Fauzan Khairi Che Harun (Member, IEEE) received the B.Eng. degree in electrical-electronics engineering from Universiti Teknologi Malaysia (UTM) in 2003, and the M.Sc. degree in advanced electronic and the Ph.D. degree in engineering from the University of Warwick, U.K., in 2005 and 2010, respectively. He is currently a Senior Lecturer with the Faculty of Engineering, UTM. His research interests are mainly biomedical electronics, biological inspired micro-system, and electronic nose system.



Leny Yuliati received the B.Sc. degree from Gadjah Mada University in 2000 and the M.Eng. and D.Eng. degrees from Nagoya University, Japan, in 2005 and 2008, respectively. She currently works as a Principal Investigator with the Ma Chung Research Centre for Photosynthetic Pigments, Universitas Ma Chung, Indonesia. Her research interest is in material chemistry for heterogeneous (photo) catalysis.



Dedy H. B. Wicaksono (Member, IEEE) received the B.Eng. degree in engineering physics from Institut Teknologi Bandung, Indonesia, in 1998, the M.Eng. degree in biological information engineering from the Tokyo Institute of Technology, and the Ph.D. degree in microelectronics from TU Delft in 2008. He currently works as an Assistant Professor and the Head of the Department of Biomedical Engineering, Swiss German University (SGU), Indonesia. His research interest is in textile-based biomedical devices.